Informes Técnicos Ciemat 833
septiembre, 1997

Results obtained with a Drift Chamber Prototype in the CERN H2 test beam area

J. Berdugo
M.Cerrada
N. Colino
P. Ladrón de Guevara
J. Mocholí
L. Romero

Departamento de Fusión y Partículas Elementales

Toda correspondencia en relación con este trabajo debe dirigirse al Servicio de Información y Documentación, Centro de Investigaciones Energéticas, Medioambientales y Tecnológicas, Ciudad Universitaria, 28040-MADRID, ESPAÑA.

Las solicitudes de ejemplares deben dirigirse a este mismo Servicio.

Los descriptores se han seleccionado del Thesauro del DOE para describir las materias que contiene este informe con vistas a su recuperación. La catalogación se ha hecho utilizando el documento DOE/TIC-4602 (Rev. 1) Descriptive Cataloguing On-Line, y la clasificación de acuerdo con el documento DOE/TIC.4584-R7 Subject Categories and Scope publicados por el Office of Scientific and Technical Information del Departamento de Energía de los Estados Unidos.

Depósito Legal: M-14226-1995
NIPO: 238-97-001-5
ISSN: 1135-9420

Editorial CIEMAT

CLASIFICACIÓN DOE Y DESCRIPTORES

440104; 662110
MUON DETECTION; MUONS; WIRES; DRIFT CHAMBRES; CERN; ACCELERATORS

Results obtained with a Drift Chamber Prototype in the CERN H2 test beam area

Berdugo, J.; Cerrada, M.; Colino, N. Ladrón de Guevara, P.; Mocholí, J. and Romero, L.

42 pp. 28 figs. 6 refs.

Abstract:

The performance of a small size prototype of the CMS barrel muon chamber detector has been studied in a test beam. Results on chamber efficiency, drift velocity and single wire resolution, under different experimental conditions are presented. The effects of the magnetic field on the chamber behaviour are also discussed.

Resultados obtenidos con un prototipo de cámara de deriva en la zona H2 del CERN con haces de muones

Berdugo, J.; Cerrada, M.; Colino, N. Ladrón de Guevara, P.; Mocholí, J. and Romero, L.

42 pp. 28 figs. 6 refs.

Resumen:

Las prestaciones de un prototipo de pequeño tamaño de las cámaras de muones del detector central del experimento CMS han sido estudiadas mediante su exposición a un haz de partículas. Se presentan los resultados obtenidos sobre eficiencia de la cámara, velocidad de deriva y resolución por hilo, en diferentes condiciones experimentales. se describe también el efecto del campo magnético en el comportamiento de la cámara.

1 Introduction

A small size prototype of a CMS barrel muon chamber station was built at CIEMAT during the first four months of 1996. One of the aims was to evaluate assembly procedures in view of future chamber mass production. A detailed description of the prototype design and the construction process can be found in [1]. The present report is devoted to another important goal, namely the study of the prototype performances in a high energy muon test beam.

General features of the CMS barrel muon chambers are described in [2]. Although still some details have to be worked out in the final detector design, the tracking and triggering requirements of these chambers are essentially known. Therefore prototypes are very useful in order to test wether or not these requirements can be met.

The CIEMAT prototype was installed in the H2 test beam area in the CERN-SPS North Hall and data were taken during two periods in 1996. Other prototypes, made by our collaborators from Aachen and Padova, were also taking data in the same area. Some results of this common effort concerning chamber noise, efficiency, drift velocity and resolution, in the absence of magnetic field, have been already submitted for publication [3].

This report contains a full summary of the results obtained with the CIEMAT prototype. It is organized in the following way:

In section 2 some basic information about the prototype is provided. The experimental set up and the data taking conditions in the H2 test beam area are described in section 3. General features of the data processing and the analysis are presented in section 4. Section 5 deals with the results obtained without magnetic field when having the chamber perpendicular to the beam direction. The effects of changing the angle of incidence are described in section 6. Results with magnetic field are presented in section 7. We draw some conclusions in section 8.

2 Description of the CIEMAT prototype

As shown in figure 1, the drift cell has a 40 mm x 13 mm rectangular section with a single stainless steel 50 microns diameter anode wire in the center. The wire length is about 500 mm. Top and bottom planes are made of 2 mm thick aluminium sheets, connected to ground, and insulated from aluminium I beam cathodes by Lexan strips 0.5 mm thick. Field uniformity is improved by adding two copper strip electrodes 14 mm wide, mylar backed for insulation purposes, one above and another below the wire.

Four layers, each having 12 such cells, make a quadruplet (also called a su-

perlayer) as shown in figure 2. The prototype included 4 quadruplets. The first and the third quadruplet have their wires parallel and along the vertical direction (we will refer to them as vertical superlayers). The second and the fourth quadruplets have also their wires parallel but in a direction perpendicular to the other two quadruplets (we will refer to them as horizontal superlayers). In between the second and the third quadruplet there is a honeycomb panel, 9 cm thick, which provides some additional mechanical stiffness and increases the lever arm for tracking.

Superlayer assembly was described in detail in [1], as well as the simple electronics on the chamber (inside the gas volume). We used old preamplifiers and discriminators from L3 muon chambers [4] to process the signals coming from the anode wires. Preamplifiers were located outside the chamber boxes, about 30 to 40 cm away from the wire ends. The read out was done with multi-hit LeCroy-2277 TDC's. All superlayers were gas tight and operated with the same gas mixture : Argon (85%) and CO_2 (15%).

The first superlayer we produced was transported to CERN end of April 1996. Setting up was rather succesful and it was operational in a few days. Although the purpose of this exercise was mainly to find out any possible problems showing up during installation in the test beam area, we were able to take useful data operating in a parasitic way during a whole week (beginning of May). We will refer to this period as "May data". In June, the complete prototype (4 superlayers) was installed and we had a two weeks period of data taking. Most of the results presented in this report come from the analysis of the "June data".

3 Experimental set up

The H2 test beam area in the CERN-SPS North Hall can provide secondary muon beams in a rather high energy range (order of 200 to 300 GeV). Intensities could be adjusted so that not more than a few thousand muons could go through a typical chamber region of 10 x 10 cm squared in a spill of about 2 seconds. There were spills every 15 seconds.

Our prototype was installed inside the M1 superconducting magnet (the EHS magnet) which could provide up to a 3 Tesla field in a horizontal direction perpendicular to the beam. A simple trigger using scintillator counters was used to define good beam tracks and also to give T_0 information.

We took data at different voltage settings, the reference values being: $V_{wire} = 3300V$, $V_{strip} = 1500V$, $V_{cathode} = -1500V$. The effect of having different discriminator voltage settings was also studied, being 64 mV (equivalent to a charge of 4 fC) the reference value.

At CMS there will be a big range of possible angles of incidence (with respect

to the direction perpendicular to the wire planes) of muons crossing the barrel chambers. Therefore it is important to study the performance of the chamber as a function of this angle. In June, our prototype was mounted on a special fixture which allowed a rotation around a vertical axis. Data were taken at different angle values (0, 14, 24, and 34 degrees). In May also a rotation around a horizontal axis was possible.

The influence of the magnetic field B in the performance of the chamber has also been studied. Data were taken for several values of B (up to 1 Tesla) and different angles between B and the wire planes.

About 90 runs, 60000 events each in average, were processed in May, and 250 runs, 40000 events each in average, were processed in June.

4 Data analysis

During data taking, a monitoring program developped by us allowed to check, online, hit rates and TDC spectra for each channel. This was useful to detect inmediately variations in noise levels or other problems which could influence data quality. The detailed data analysis was however performed offline.

4.1 Noise and multiple hits

The amount of random noise can be easily extracted from the data, as shown in figure 3, by looking at hits outside the time window corresponding to physical hits (TDC multihit capability allows to record hits within a time range of 64 microseconds, but hits corresponding to a triggered muon track will only occur during several hundreds of nanoseconds after T_0. A typical value of 500 Hz per channel was usually found, but depending on data taking conditions it could become up to a factor 4 worse. This is however not a problem for track reconstruction: the probability of a random hit occuring within the drift time of a physical hit is, for the usual test beam trigger rate, smaller than 0.1%.

Typical multiple hit rate (fraction of hits which were accompanied by at least another hit in the same cell) was of the order of 10%. Some of these extra hits have a physical origin, but a big part of them are correlated noise produced by the signal processing electronics. For track reconstruction purposes all hits inside the same cell, and inside a reasonable time window, were considered as good hit candidates, and the combination of them (one hit per layer) giving the best χ^2 was retained. Usually, in almost 90% of the cases, the first hit is the one providing the best χ^2. The extra 10% of multihits can be understood by the presence of delta rays produced when the muon goes through the aluminium plates.

4.2 T_0 calibration

A system of test pulses induced onto the wires, such as the one used in the L3 muon detector in order to ensure relative T_0 calibration [5], was applied to our prototype. Therefore, possible effects coming from different cable lengths, as well as other channel dependent electronic effects, are properly taken into account. The system is precise to better than 1 nanosecond. Special T_0 runs were taken at least once a day for these calibration purposes. By analysing these runs we obtained a global T_0 value and a time dependent data base file with T_0 corrections for each individual channel.

A global T_0 can also be extracted directly from the data using the TDC spectrum as sketched in figure 4. We have applied several methods to determine T_0 run by run, the aim being to monitor any possible run dependent effects. The evolution with time of this global T_0 value is shown in figure 5 for the whole data taking period. Small fluctuations (only rarely exceeding of 1 nanosecond) around a rather stable central value can be seen.

4.3 Pattern recognition

In each superlayer independently a simple scheme of pattern recognition was applied in order to extract, without any fitting, "track" candidates. In a first go all possible configurations of "track" types (a total of 8 different types were identified) having 4 hit cells (one in each of the 4 layers) were tried. In case of not finding any track of this kind, a second try was performed allowing also 3 hit cell topologies. Tracks having hits in 4 and in 3 layers were used, as explained below, in order to determine single wire efficiencies in each superlayer.

As an example, figure 6 shows one event which has "track" candidates in the 4 superlayers of the prototype.

4.4 Efficiency determination

A selected subset of tracks found in the pattern recognition process is used to determine single wire efficiency. Selection cuts are applied just to ensure that the track has a slope compatible with the average beam slope of the run. In case of having several tracks in the same event, only the track having the best χ^2 is considered (see the track fitting section).

Single wire efficiency can be extracted from two numbers: C_1, which accounts for the number of times a cell belonging to the track has a hit (as it should), and C_2, which accounts for the number of times there is no hit in that cell. If one defines $C = C_1/(C_1 + C_2)$, it is straigthforward to get an expression for the single wire efficiency (taking into account the 4 layers configuration of a superlayer): $Eff = (3 - 4 * C)/(2 - 3 * C)$.

Overall superlayer efficiency is obtained by averaging the efficiency values obtained in each cell. Dead cells (there were a few disconnected wires in the prototype) are not included when calculating the overall efficiency.

4.5 Track fitting

For those tracks found in the pattern recognition process a fit to a straight line was performed. The aim of this fit was just to identify the hits associated to the track and to resolve left-right ambiguities. Therefore all possible combinations were tried and the one giving the best χ^2 was retained. The Y coordinate of each point (the distance to the wire) is calculated from the drift time T (in nanoseconds) of the corresponding hit in each layer by just applying the simple formula: $Y = v * (T - T_0)$, v being the average drift velocity. As sketched in figure 7, a good drift velocity value will ensure a flat sagitta distribution.

As discussed below, drift velocity may change from run to run. Therefore the first time a run is analysed a value of 55 μ/ns is used in the fit. As a result of the analysis, a drift velocity value is obtained as explained in the next section and we update a file with this new value so that it will be used in subsequent analysis of the same run. This procedure can be iterated several times. In any case, track fitting results are not very sensitive to the actual value of drift velocity used (provided that it is not very different from the real one).

Typical distributions of fit residuals are shown in figure 8. They are well centered around 0 and have sigma values in the range 150 to 170 microns.

4.6 Drift velocity measurements

After track fitting we know the drift times of the associated track hits (either 4 hits or 3 hits per track). On an event by event basis, the maximum drift time T_{max} can be obtained by just adding hit times from two adjacent layers. For perpendicular tracks this value would correspond to a drift distance of 20 mm (half a cell size). From a gaussian fit to the T_{max} distribution it is possible to determine the mean value $< T_{max} >$. Assuming then a constant drift velocity v, we can calculate v by simply doing $v = 20000/ < T_{max} >$ (in μ/ns). Effects of angles of incidence different from zero can be cancelled out by just averaging mean values of T_{max} obtained with data from left half cells and data from right half cells separately. Since there are several combinations of adjacent layers several values of T_{max} can be obtained for each track. Any of them can in principle be used in the calculation, but we decided to use the one obtained by just averaging all of them.

A constant drift velocity is equivalent to assume a linear relation between time and distance to the wire (space-time relation). This is in fact a very important ingredient in the chamber performance when considering the mean timer method [6] which will be used for triggering purposes. Mean timers MT_1 and MT_2 are

defined as $MT_1 = T_2 + 0.5 * (T_1 + T_3)$ and $MT_2 = T_3 + 0.5(T_2 + T_4)$, T_i being the drift time corresponding to the i layer of the superlayer. Typical mean timer distributions are shown in figure 9.

As described below, we have checked how the data agree with such an assumption under different conditions. Deviations from linearity have been studied as a function of the distance from the wire.

4.7 Resolution measurements

Single wire resolution has been evaluated in two ways. First, using the width of the T_{max} distribution (or the meantimer distributions, MT_1 and MT_2). The second method is to use the distribution of residuals from the straight line fit. This method allows also to study how resolution changes as a function of the distance from the wire.

Both methods give only rough estimates of the resolution, but the results obtained are compatible and good enough to understand the qualitative behaviour of the resolution as a function of different run conditions.

The ideal way of measuring resolution would be to have external tracking detectors providing a good reference to compare with the actual coordinates measured by the prototype. This was not available during the data taking period. However we have taken advantage of the fact of having several superlayers, which allows to extrapolate track information from one to another thus improving our reconstruction of the muon beam trajectories.

5 Results for $B = 0$ and normal incidence

These data can be used first to check the alignment between the different superlayers. As shown in figure 10, misalignment in X and Y is not bigger than 0.2 mm. Vertical superlayers are parallel to 0.1 mrads and horizontal superlayers are parallel to 0.7 mrads.

Beam slopes are measured independently in each superlayer. Typical resolutions, as shown in figure 11 are of the order of 6 or 7 mrads. A much better beam slope resolution can be achieved after track matching between superlayers (see also fig 11). The values obtained are in fact compatible with the expected beam spread of 1.2 mrads.

5.1 Single wire efficiency

As shown in figure 12, efficiency is not very much dependent on the threshold provided we are below 8 fC. With higher threshold values inefficiency increases

very significantly. At the default value, 4 fC, the inefficiency is located mainly near the I beams. Removing this region we get always efficiency values which are bigger than 99%.

Figure 13 shows how the efficiency changes as a function of the distance to the wire (the region very close to the I beam has not ben included in the plot). There is a clear peak at around 15 mm away from the wire. Although a detailed montecarlo simulation has not yet been made, a possible explanation of such an effect could be provided by the peculiar electric field shape inside the drift cell.

In order to study the effect of different voltage settings we can define, as explained in [3], an effective voltage V_{eff} in the following way:

$V_{eff} = (V_{wire} - V_{strip}) + 0.16V_{strip} - 0.037 * V_{cathode}$

We show in figure 14 the efficiency values obtained as a function of V_{eff}. A plateau with very high efficiency values is reached when V_{eff} becomes bigger than 2100 Volts. The main contribution to V_{eff} comes from the term $V_{wire} - V_{strip}$, which we will call from now on V_{ampl}. Good efficiency is guaranteed when V_{ampl} is 1800 Volts.

5.2 Drift velocity

The measured drift velocities increase with the value of V_{ampl} as shown in figure 15. For the default voltage settings, drift velocity is $55.7\mu/ns$. It also increases with V_{drift}, defined as $V_{strip} - V_{cathode}$, but only very slightly (see figure 16). Linearity in the space-time relation is very good in this configuration of perpendicular beam tracks but it gets worse when increasing the incoming muon angle of incidence as we will show in section 6.

5.3 Resolution

As shown in figure 17, single wire resolution gets better as V_{ampl} increases. For $V_{ampl} = 1800$ Volts, or bigger, resolution is of the order of 200 microns. This is precisely the value included in the design goals for the barrel muon detector in the CMS technical Proposal [2].

6 Results for $B = 0$ at different angles of incidence

Bigger angles imply longer paths for the muon tracks and therefore more primary ionizations. Except in the region near the I beams one would then expect that efficiency can only improve when the angle increases and this is actually what

can be seen in figure 18: very small variation, the efficiency improving slightly at bigger angles.

As far as drift velocity is concerned, a rotation around the vertical direction might affect vertical superlayers, but not the horizontal ones. This is in fact what figure 19 shows: drift velocity stays roughly constant in the horizontal superlayers and increases in the vertical superlayers. The increase is approximately linear, reaching 5% at around 40 degrees. In CMS this effect should be taken into account in the trigger logic.

One would naively expect that deviations from linearity, in the the space-time relation, would become more important as the angle of incidence increases. In order to study this effect, track matching between the two vertical superlayers was made to help selecting a good subsample of beam tracks. A global fit to a straight line using the eight wires information was performed imposing the average beam slope as a constraint. Fit residual distributions have been studied in different drift time bins, or equivalently in different cell regions. This allows to estimate the deviations from linearity as a function of the distance to the wire. Results are plotted in figure 20 for the four available angles of incidence. Deviations as big as 300 microns are visible at 34 degrees, whereas they are smaller than 100 microns for perpendicular tracks.

The non linearity in the space-time relation will influence the value obtained for the single wire resolution. One should expect in principle that resolution gets worse for larger incidence angles and this is what can be observed in figure 21. Instead of looking at the global resolution shown in figure 21, one could try to understand how the resolution changes as a function of the distance to the wire. Just for this purpose we made drift time bins and calculated the resolution in each of them independently. The results are plotted in figure 22. It is still clear that resolution gets worse when the angle of incidence increases. However, resolution values as obtained from figure 22 are better than the global resolution values previously shown.

7 Results with magnetic field

The magnetic field configuration in the barrel muon chamber region of CMS will consist of two components: one perpendicular to the chamber wire planes, B_n, and another one along the Z direction (the proton beam direction), B_z. The data taken with our prototype in the test beam provide us with information to understand mainly the behaviour of the chambers under different B_z values.

For zero beam incidence angle, the electric field direction in the prototype drift cells is parallel to the magnetic field (E parallel to B) in the case of the vertical superlayers. Therefore, one would not expect big effects there. On the other hand,

horizontal superlayers have E perpendicular to B. The magnetic field will distort the drift lines as sketched in figure 23 and this might affect the performance of the chamber. We will report next on the observed efficiency, drift velocity and single wire resolution, for several values of B.

7.1 Efficiency

We show in figure 24 the variation of efficiency as a function of B. There is no visible effect for the vertical superlayers, but the efficiency goes down significantly as B increases for the horizontal superlayers. In CMS, B_z will be relatively small (smaller than 0.2 Teslas) in most of the chambers volume. However, near the edges (in between wheels and near the endcaps) B_z may reach higher values and therefore, in this region, the measured loss of efficiency has to be considered as a serious problem for the phi measuring superlayers.

7.2 Drift velocity

In figure 25, the apparent drift velocity is shown as a function of B for vertical and horizontal superlayers. Again, there is no variation observed in vertical wires, but the drift velocity decreases significantly when B increases for the horizontal wires. This effect is important at the level of trigger efficiency (because of the mean timer method [6]). A more detailed study has to be made in order to better understand the implications and optimise the performances.

7.3 Resolution

Resolution is also affected by the magnetic field in the horizontal superlayers as shown in figure 26. However it stays below 300 microns until near 0.6 Tesla (this does not represent a very serious problem), and only reaches 400 microns near 1 Tesla. For vertical superlayers it is always close to 220 microns.

7.4 Results for different angles of incidence

Rotating around the vertical axis is equivalent to introduce a B_n component (perpendicular to the wire plane). The results obtained, as far as drift velocity and resolution are concerned, have been summarized in figures 27 and 28. They are consistent with expectations from what was obtained in the case of $B = 0$ and different angles, and in the case of normal incidence with with different B values.

8 Conclusions

The data taken with the CIEMAT prototype in the 1996 muon test beam at CERN have been analysed. The quality of the data is, usually, rather good. We have been able to get information about the achieved performance of the prototype under many different conditions. The results obtained are, in general, either complementary or in good agreement with the ones obtained with other prototypes produced at Aachen and Padova (having a similar drift cell structure but each made using a different procedure, in some cases with different components and also having different electronics). This gives us confidence that the basic drift tube design is well understood.

We have measured efficiency, drift velocity, and resolution. In the absence of the magnetic field, chamber performances meet well the required specifications. There is some degradation for large angles of incidence which is visible in the resolution and in the deviations from linearity of the space-time relation. The implications have to be studied in some more detail. A more detailed evaluation has also to be done for the case with magnetic field. For high B values, the efficiency loss and the apparent drift velocity change observed for the vertical superlayers indicate potential problems in some of the angular regions to be covered by the CMS barrel muon chambers.

9 REFERENCES

1. J. Berdugo et al. Construcción de un prototipo de cámara de deriva para el experimento CMS. Report CIEMAT 828, (1997).

2. CMS Technical Proposal. CERN/LHCC 94-38, LHCC/P1, (1994).

3. M. Benettoni et al. Performance of the Drift Tubes for the Barrel Muon Chambers of the CMS Detector at LHC. Submitted for publication to Nuclear Instruments and Methods, (1997).

4. P. Rewiersma. The L3 Wire Amplifier, NH19-6112, NIKHEF, (1986).

5. P. Duinker et al. Nuclear Instruments and Methods A273 (1988), 814.

6. F. Gasparini et al. Nuclear Instruments and Methods A336 (1993), 91.

Figures

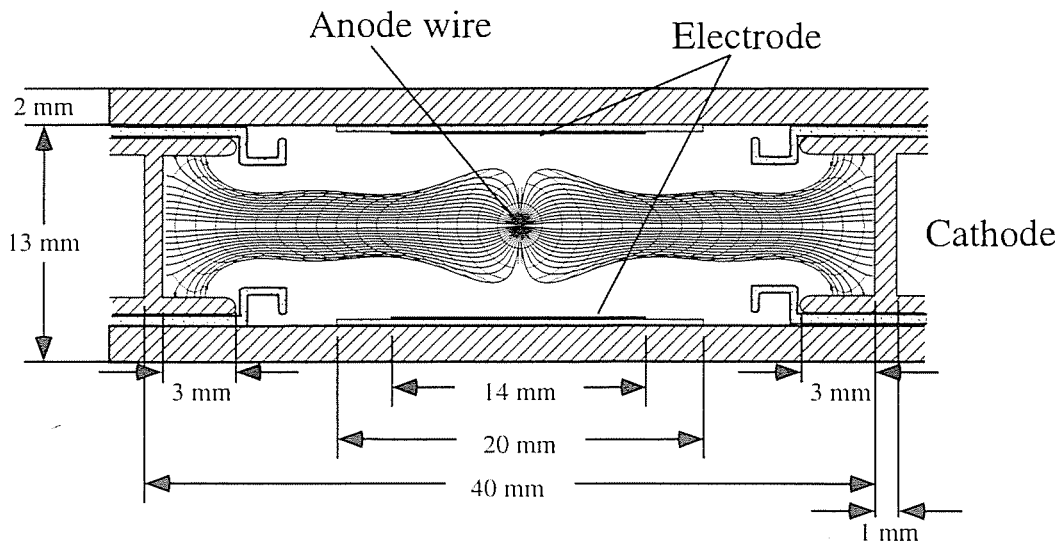

Figure 1: Sketch of the drift cell showing drift field trajectories.

SUPERLAYER WITH 4 LAYERS, 12 DRIFT CELLS EACH

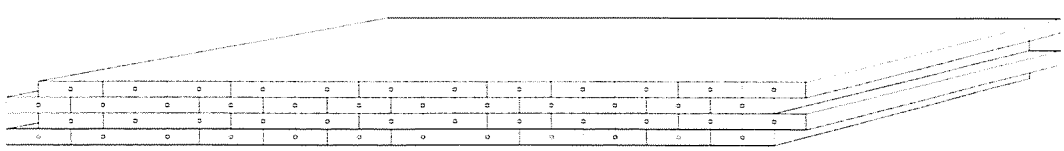

Figure 2: Sketch of a quadruplet.

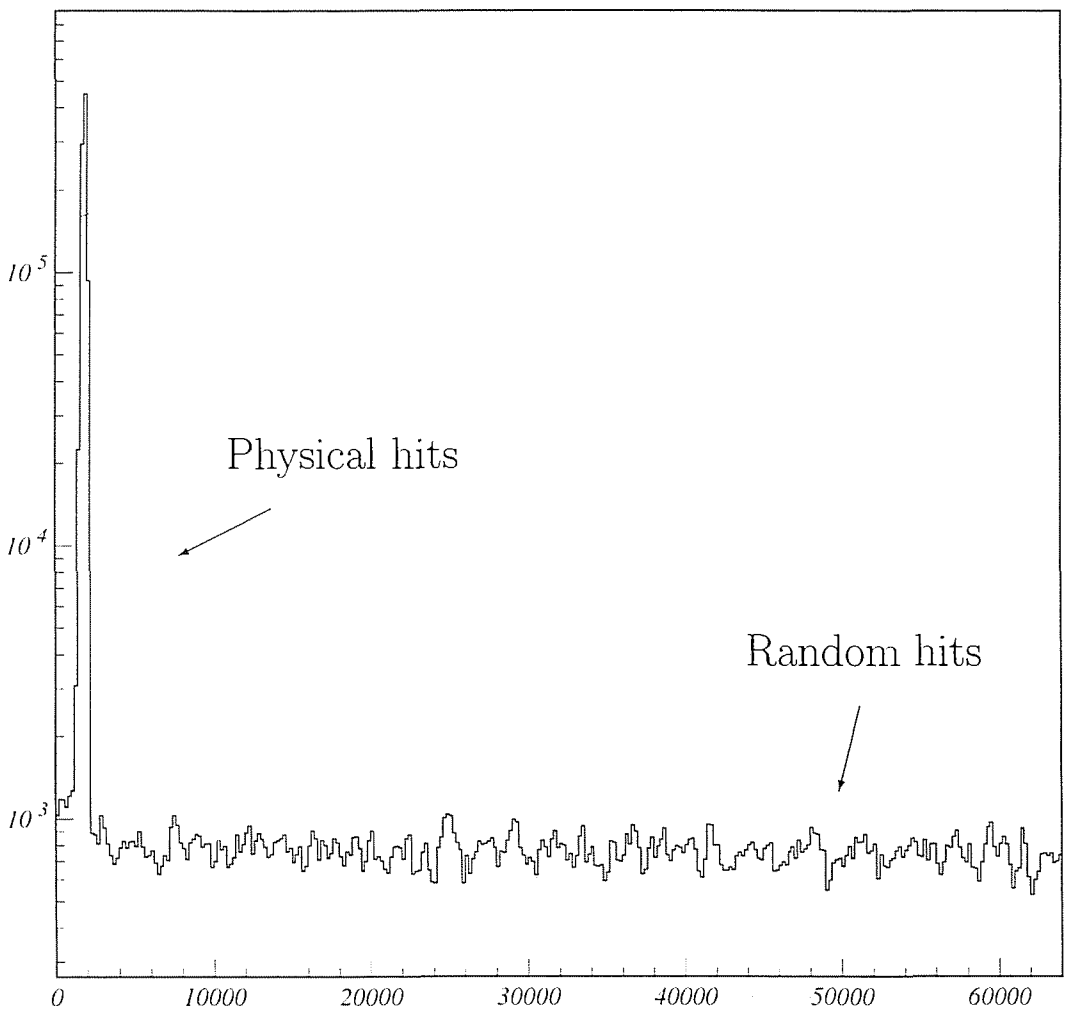

Figure 3: Distribution of times recorded by the TDC's (in bins of 200 ns). Physical hits concentrate in the peak at the left of the plot.

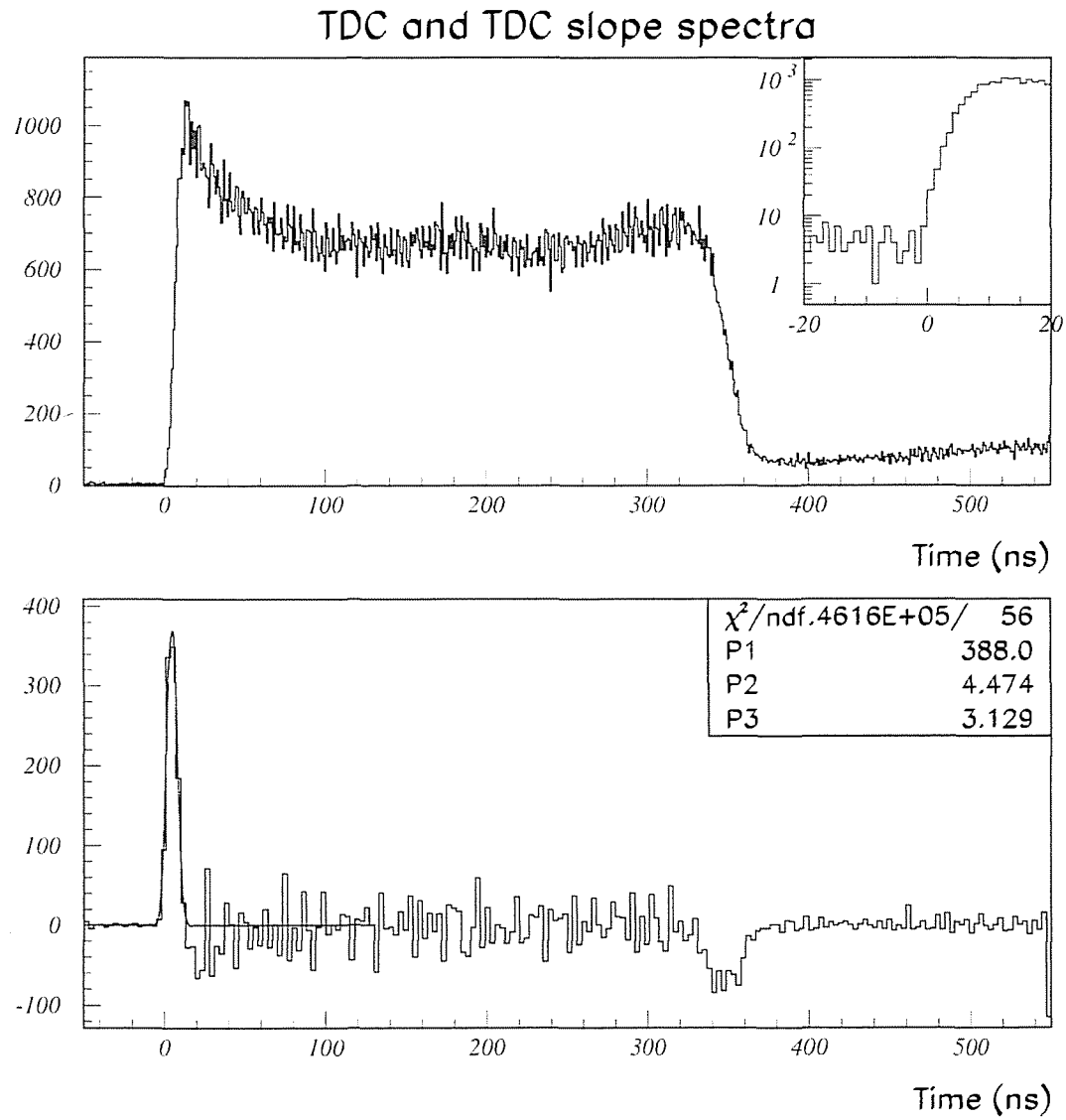

Figure 4: Typical TDC spectrum in the top graph showing as an insert the region near T_0 in logarithmic scale. The bottom graph shows how the TDC slope was also used to monitor T_0 on a run by run basis.

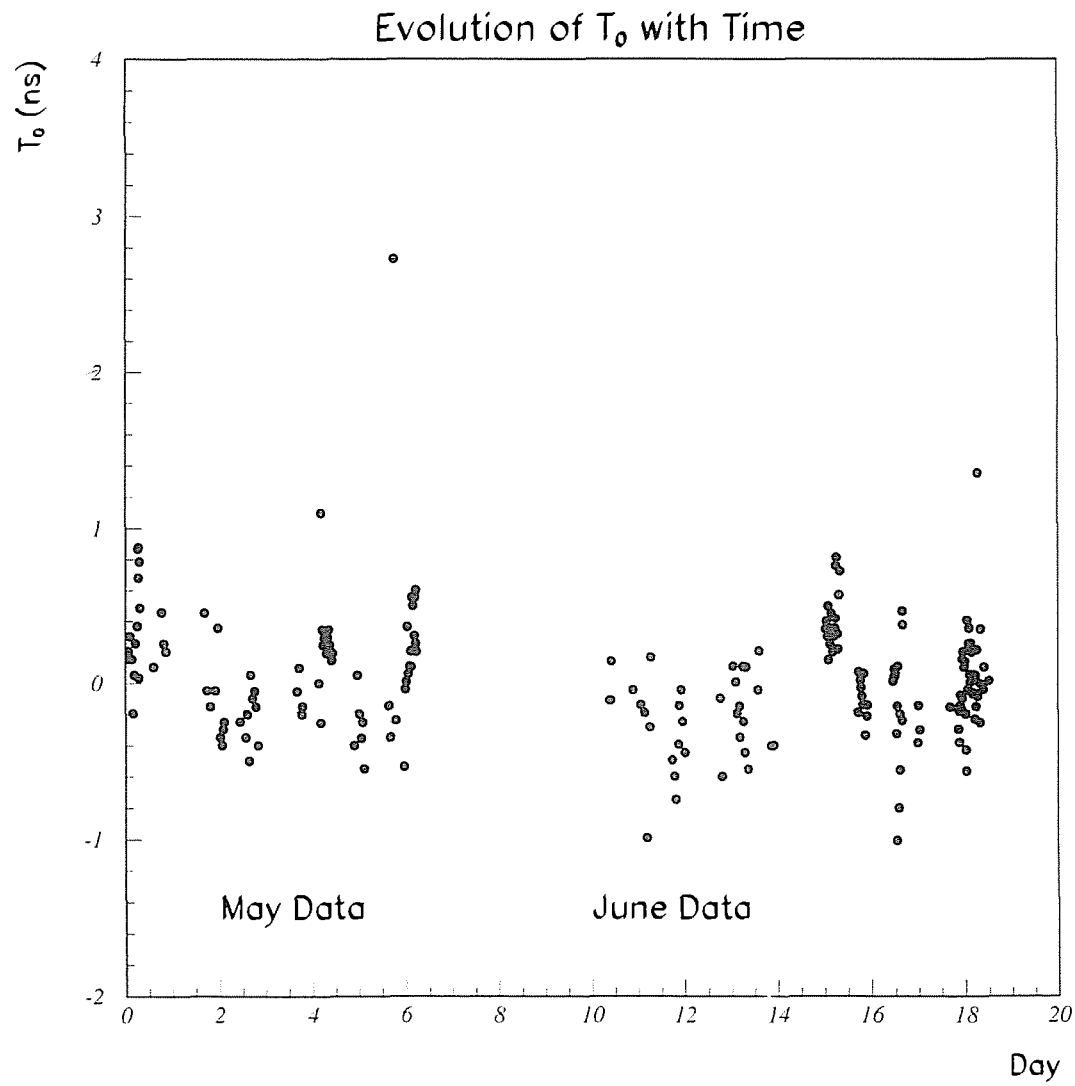

Figure 5: Variation of global T_0 during the two data taking periods.

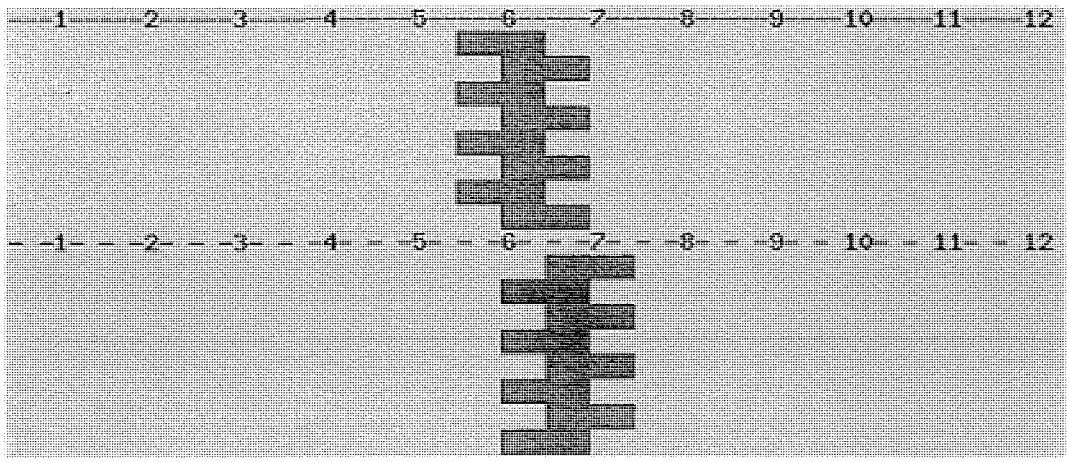

Figure 6: Track pattern defined by hit cells. This event shows a muon going through the 2 vertical quadruplets (top part) and the 2 horizontal quadruplets (bottom part). There is 1 hit cell in each layer of the 4 quadruplets.

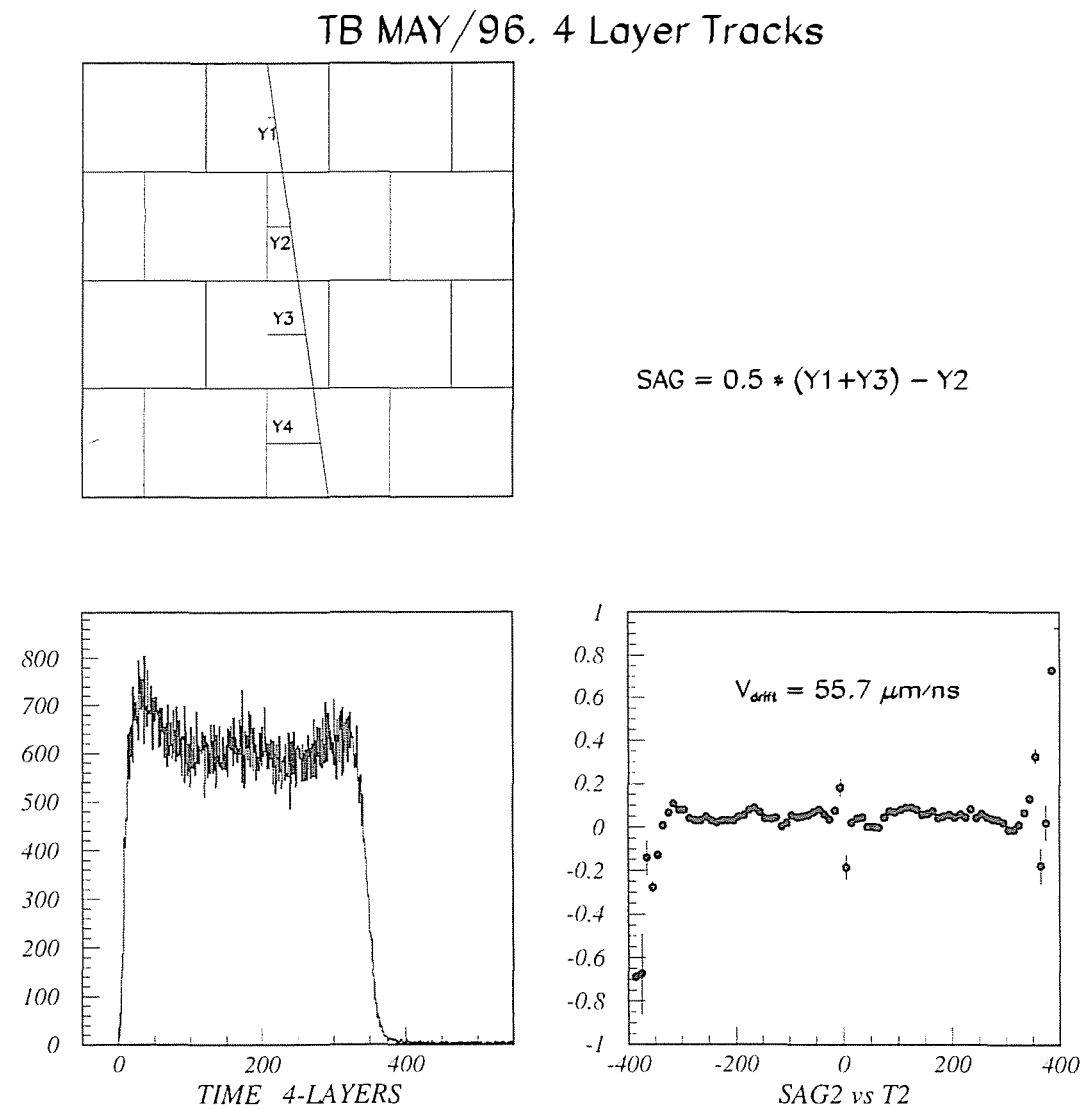

Figure 7: Schematics of track fitting within one Super Layer. Typical TDC spectrum of track associated hits (in ns). A flat sagitta distribution (as a function of drift time) corresponding to May'96 data is shown for a drift velocity of 55.7 μm/ns.

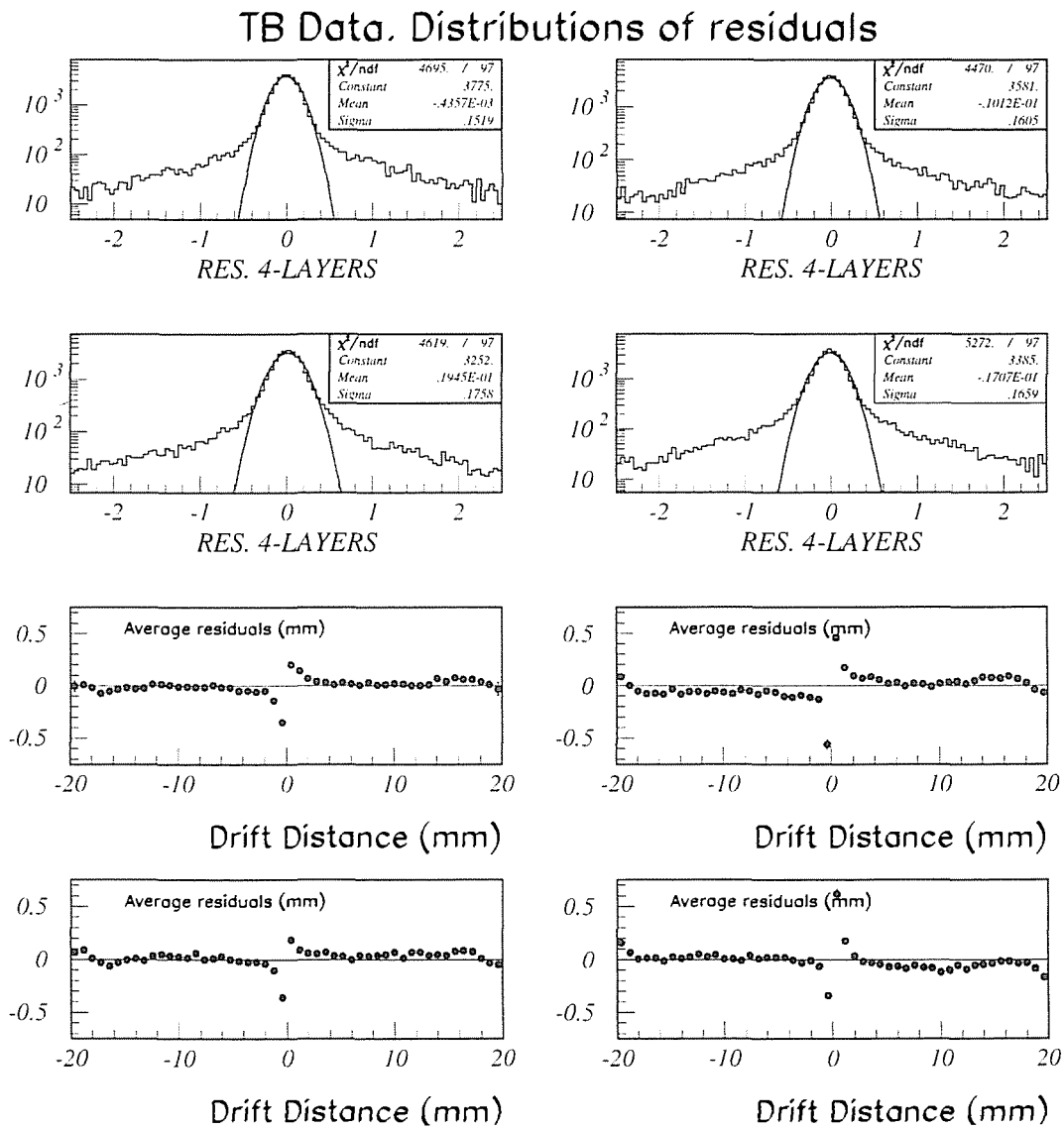

Figure 8: Distributions of residuals in mm, for a fitted track, in each of the four layers of a quadruplet. We also show residual averages versus drift length.

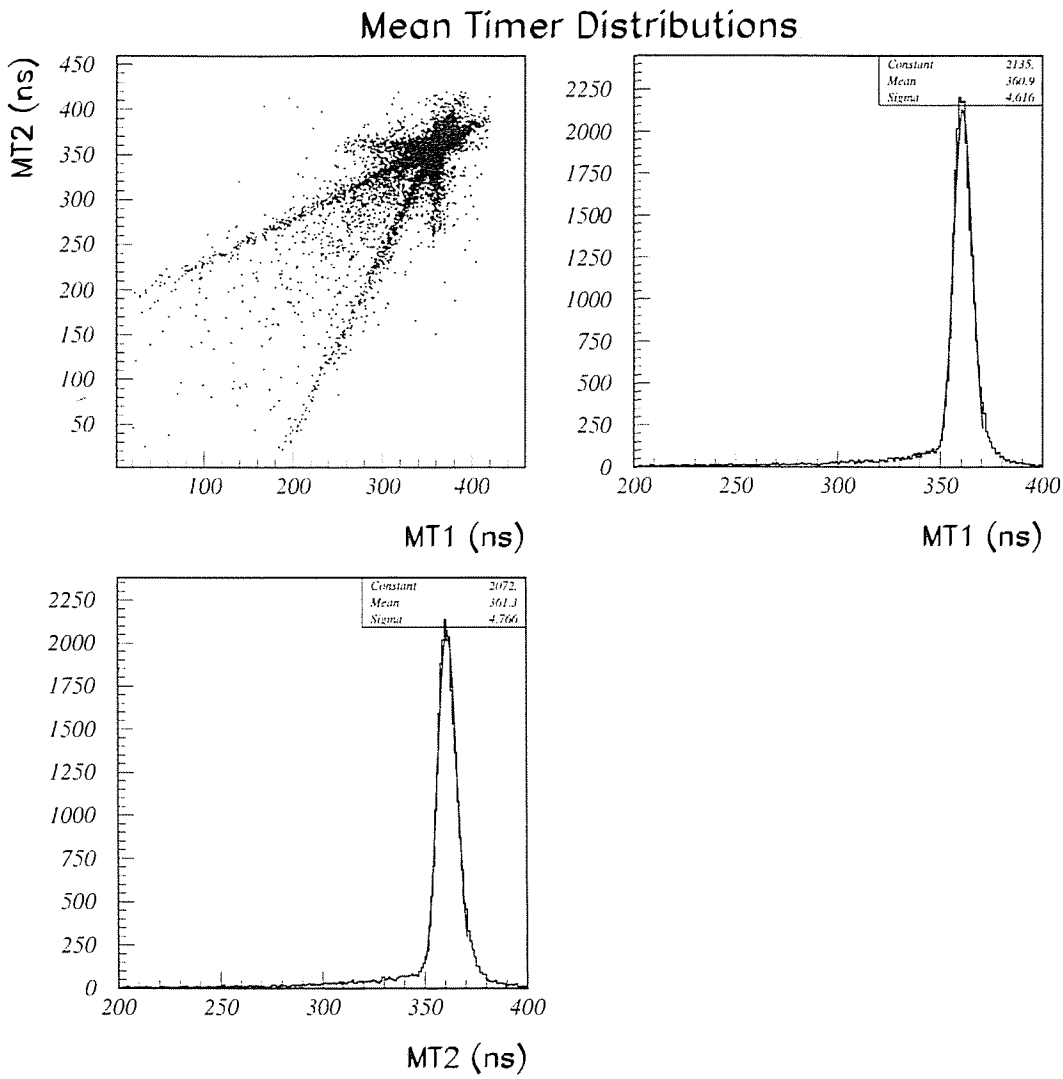

Figure 9: Typical Mean Timer distributions. A gaussian fit gives a resolution of 4.7 ns (about 210 microns)

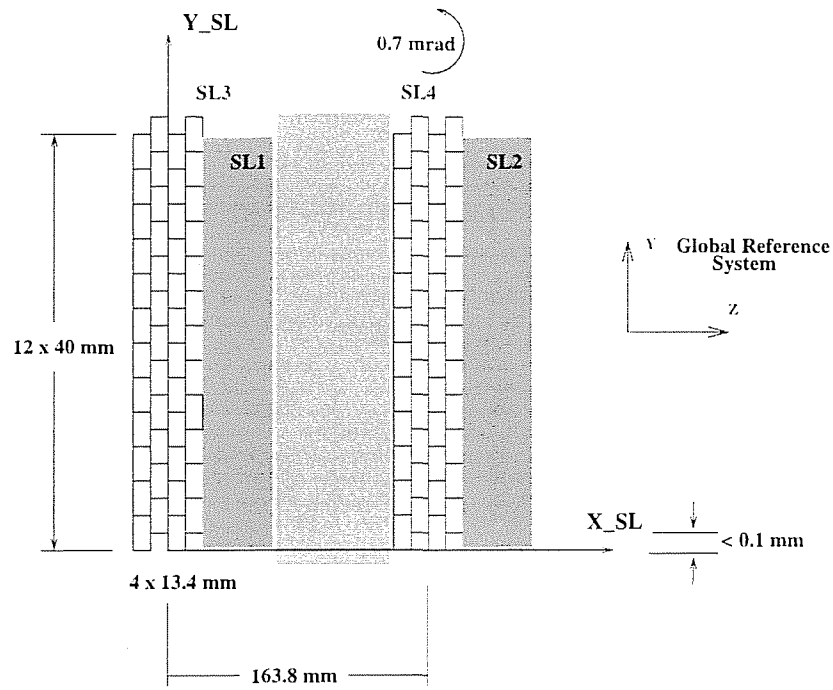

HORIZONTAL WIRES

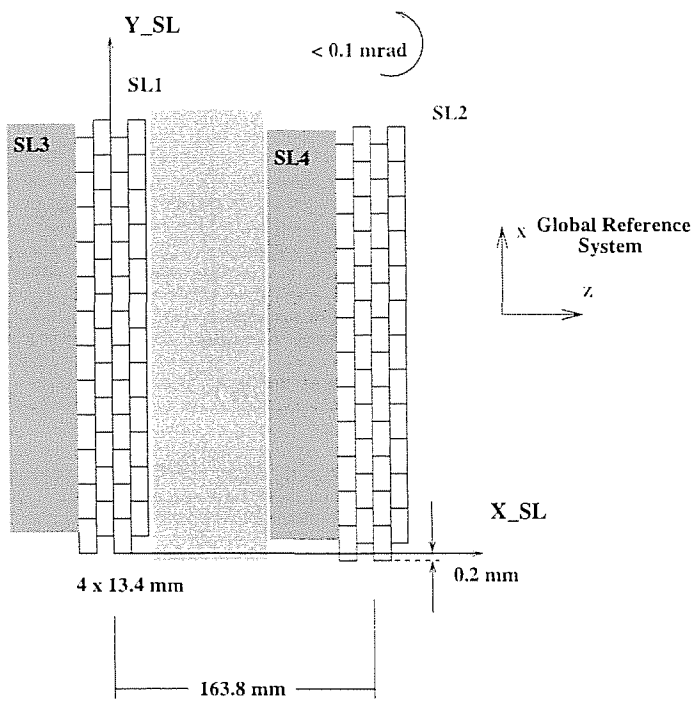

VERTICAL WIRES

Figure 10: Sketch of the CIEMAT prototype showing the 4 Superlayers (SL): two with vertical wires (wires perpendicular to B) and two with horizontal wires (wires parallel to B). From track matching between SL's we conclude that alignment in X and Y is better than 0.2 mm and parallelism is better than 1 mrad.

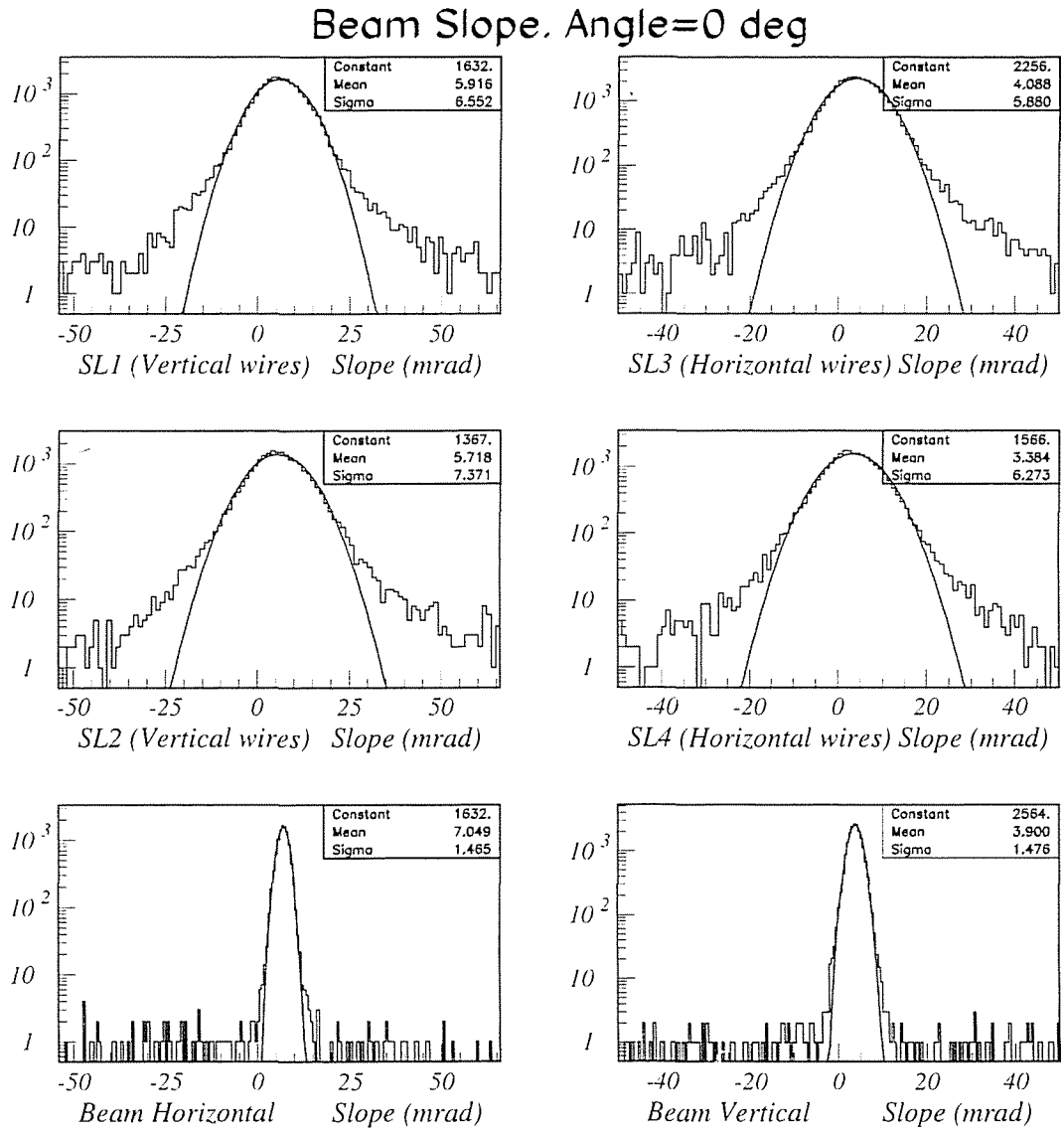

Figure 11: Beam Slopes (as measured independently in each Superlayer, SL1, SL2, SL3 and SL4). Resolutions are of the order of 6-7 mrad. After matching within SL's, the Horizontal and Vertical slopes obtained are also shown. Measured sigmas are of the order of 1.4 mrad.

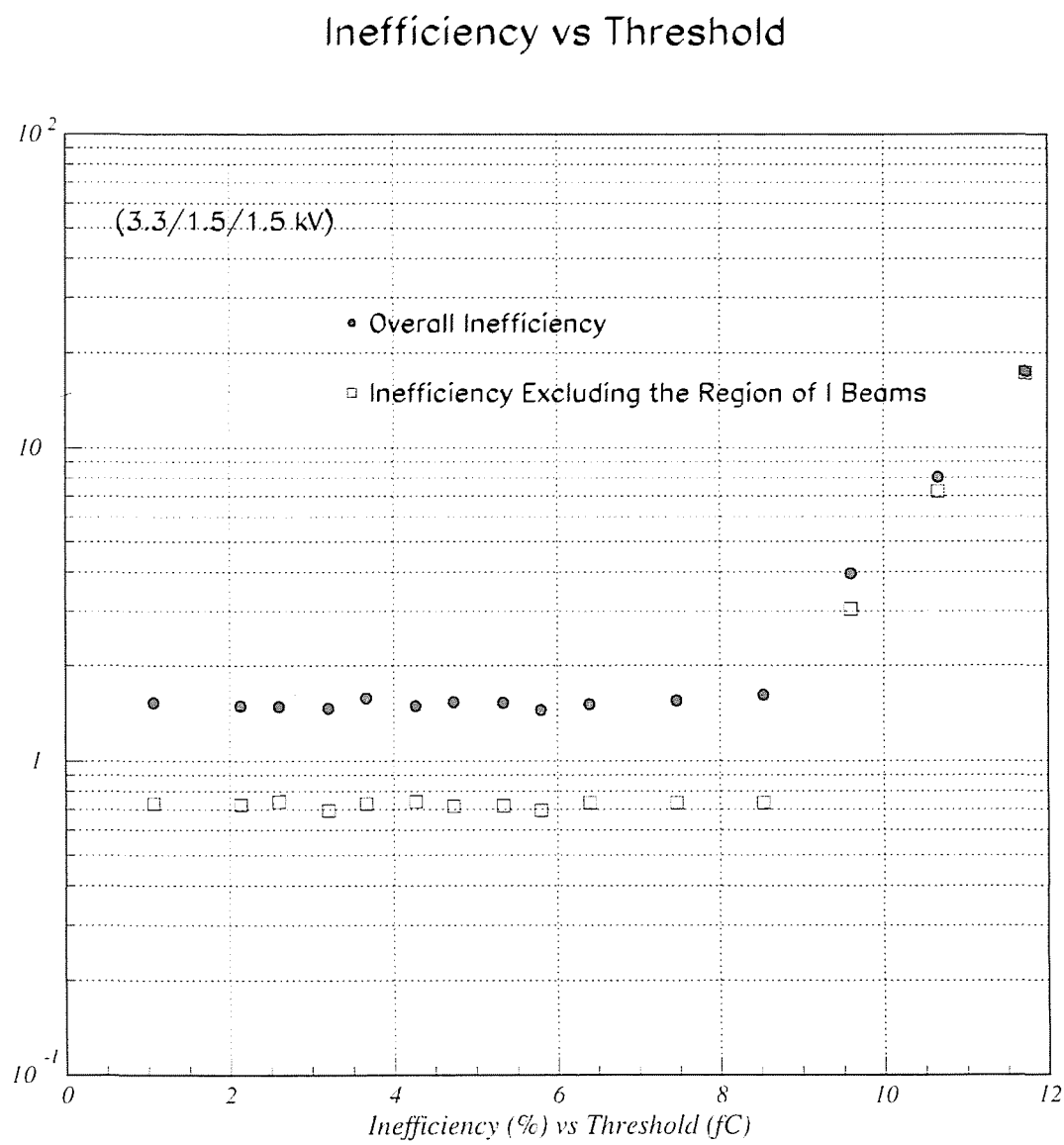

Figure 12: Single wire innefficiency as a function of the discriminating threshold.

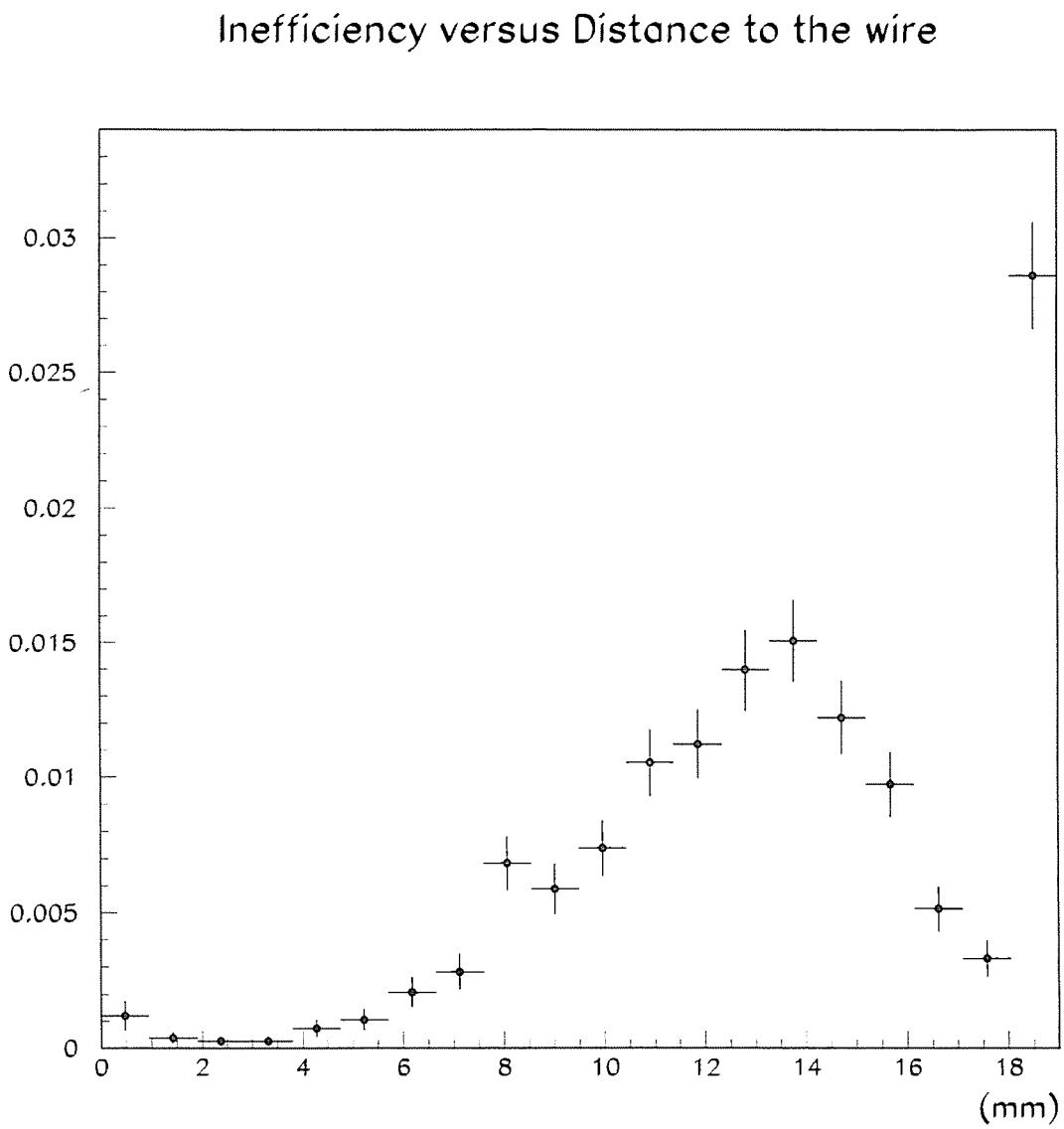

Figure 13: Inefficiency as a function of the distance to the wire.

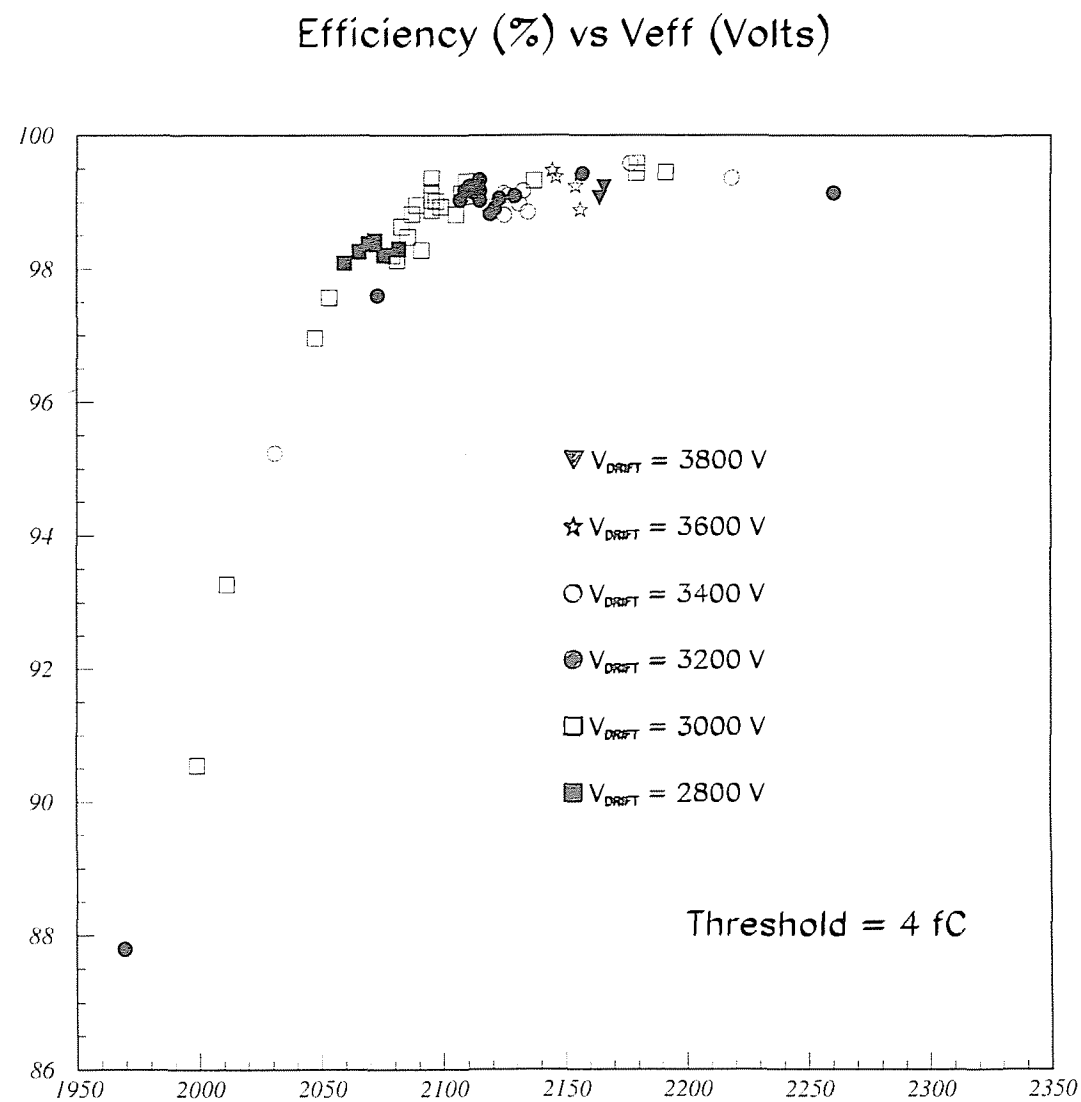

Figure 14: Perpendicular tracks. Efficiency as a function of V_{eff} (defined in the text).

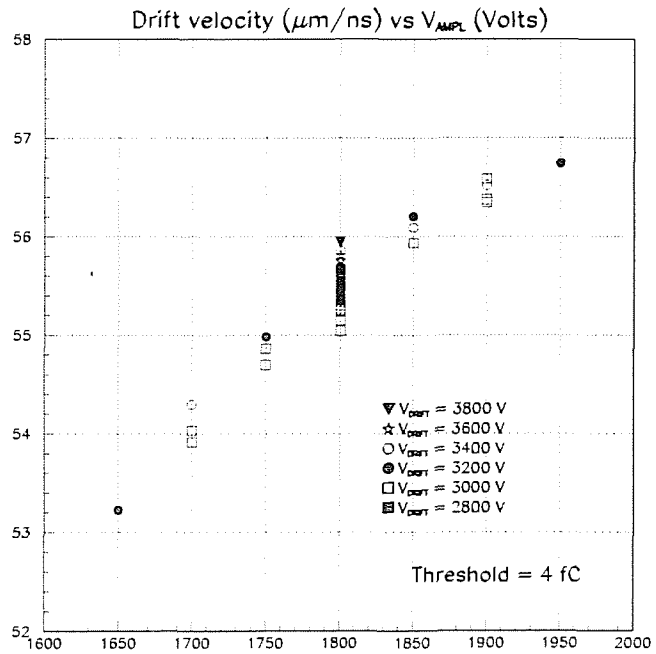

Figure 15: Drift velocity as a function of V_{ampl} (defined in the text).

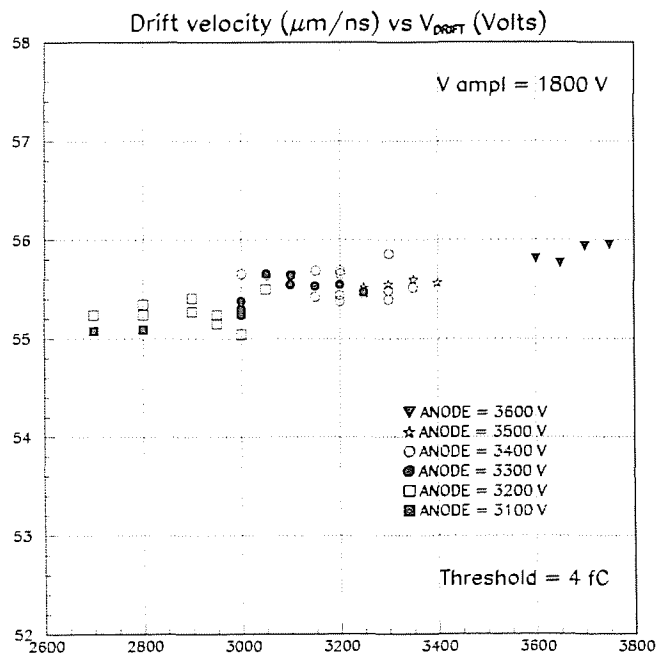

Figure 16: Drift velocity as a function of V_{drift} (defined in the text).

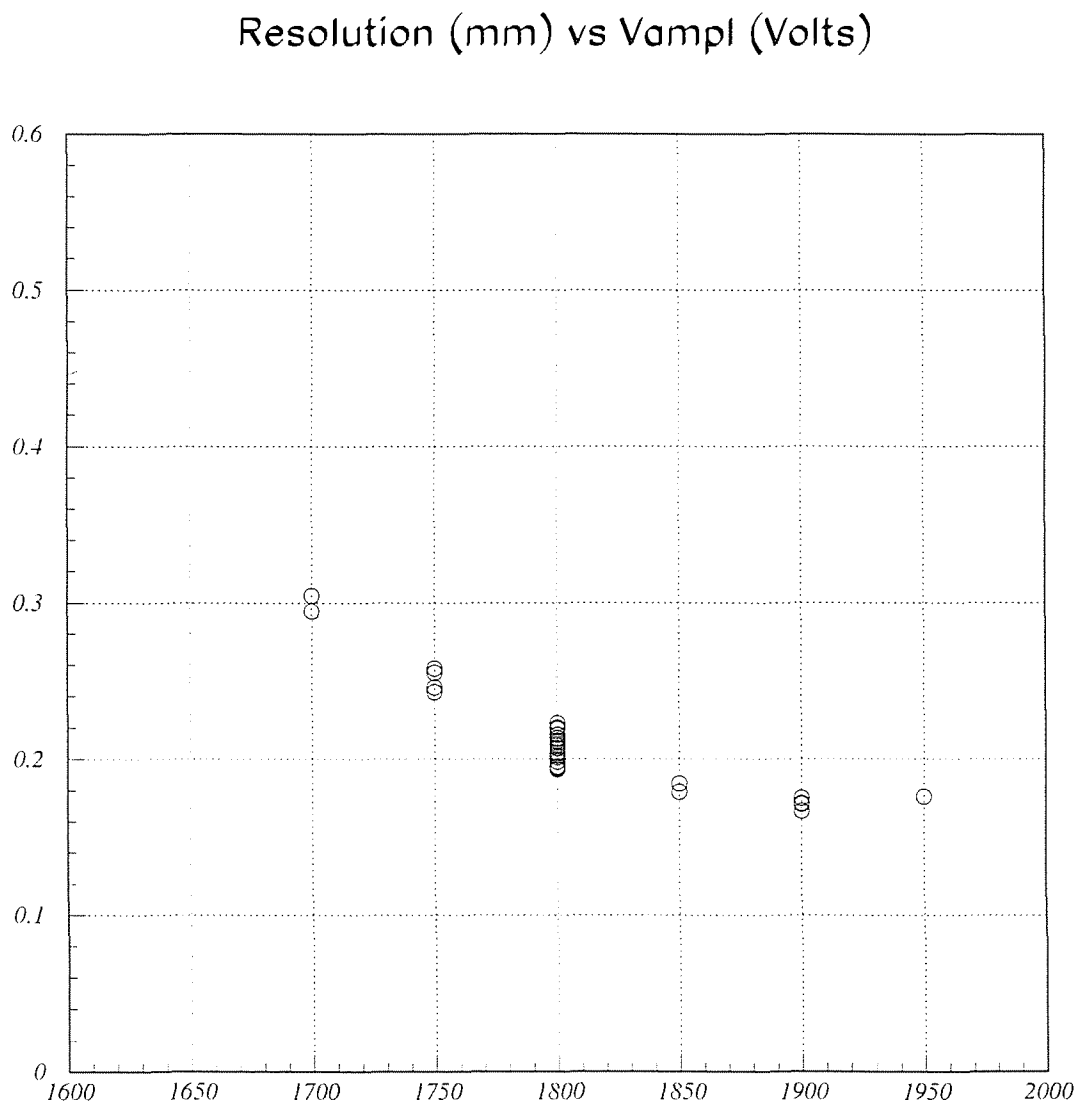

Figure 17: Single wire resolution as a function of V_{ampl} for perpendicular tracks.

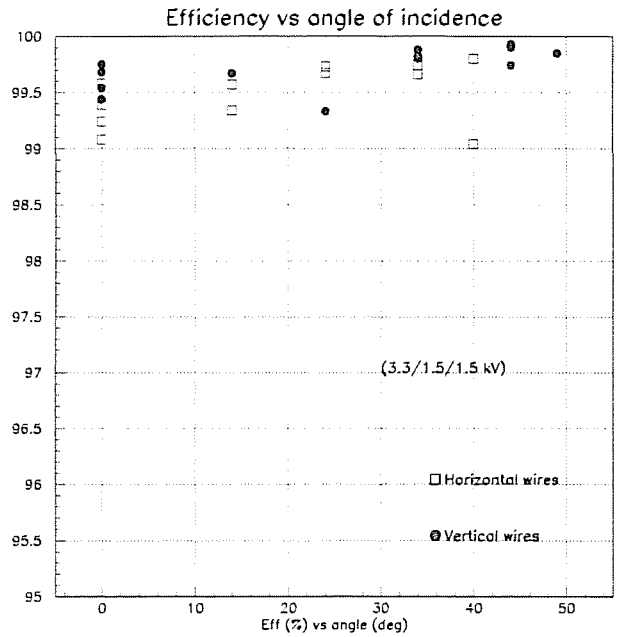

Figure 18: Efficiency for different angle of incidence. The region near I-beams has been excluded.

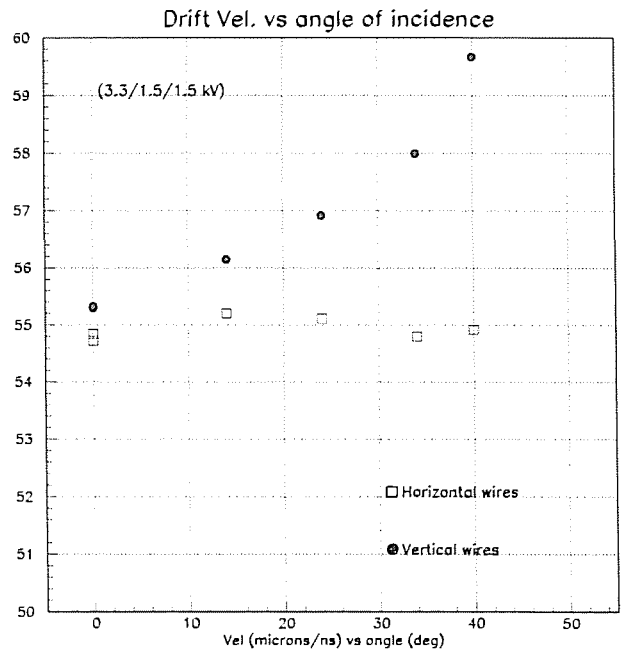

Figure 19: Apparent drift velocity as a function of the angle of incidence.

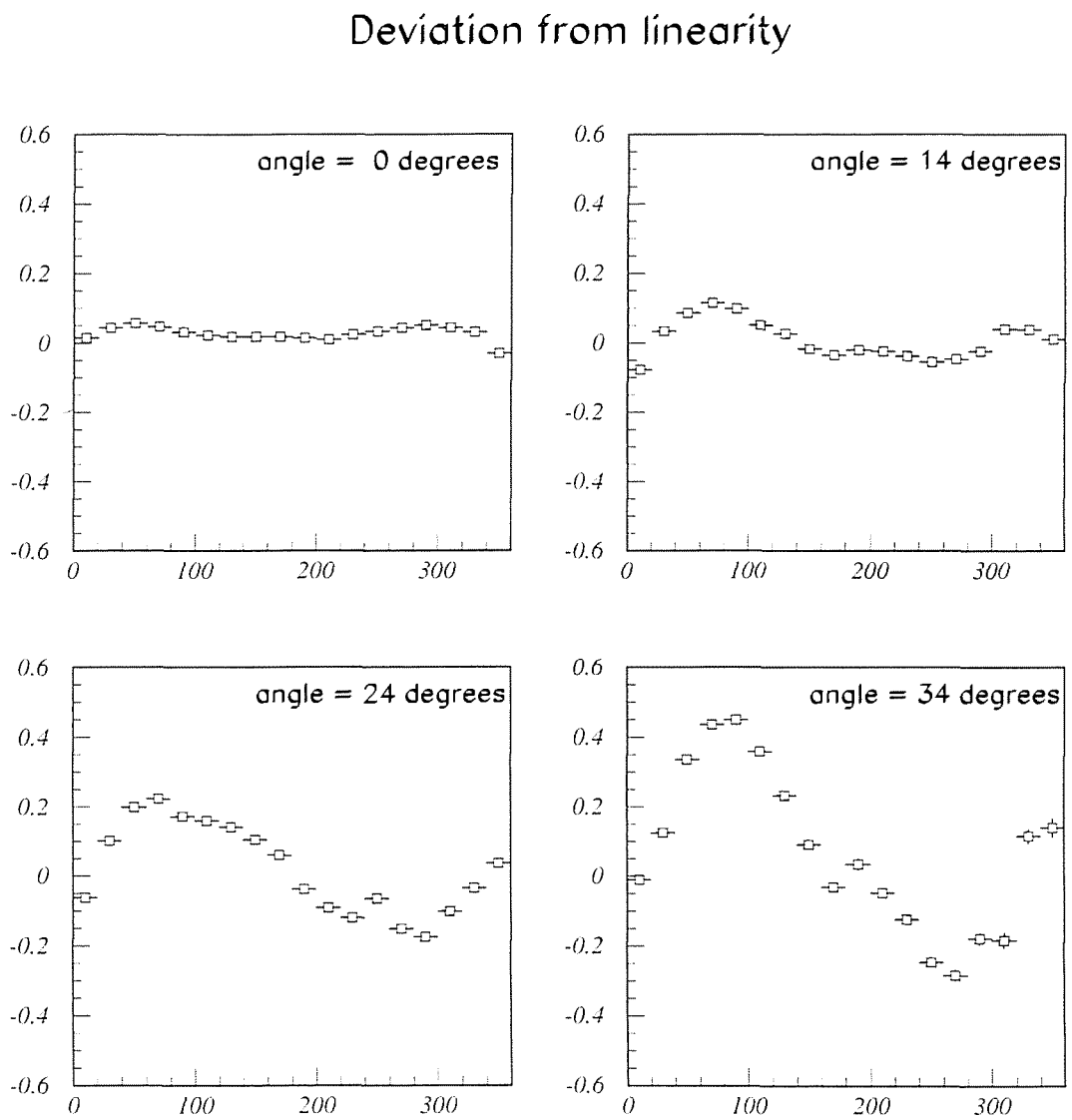

Figure 20: Deviations from linearity, in mm, as a function of the drift time, in ns, for different angles of incidence. Very minor effects can be seen for perpendicular tracks but they become more important at bigger angles.

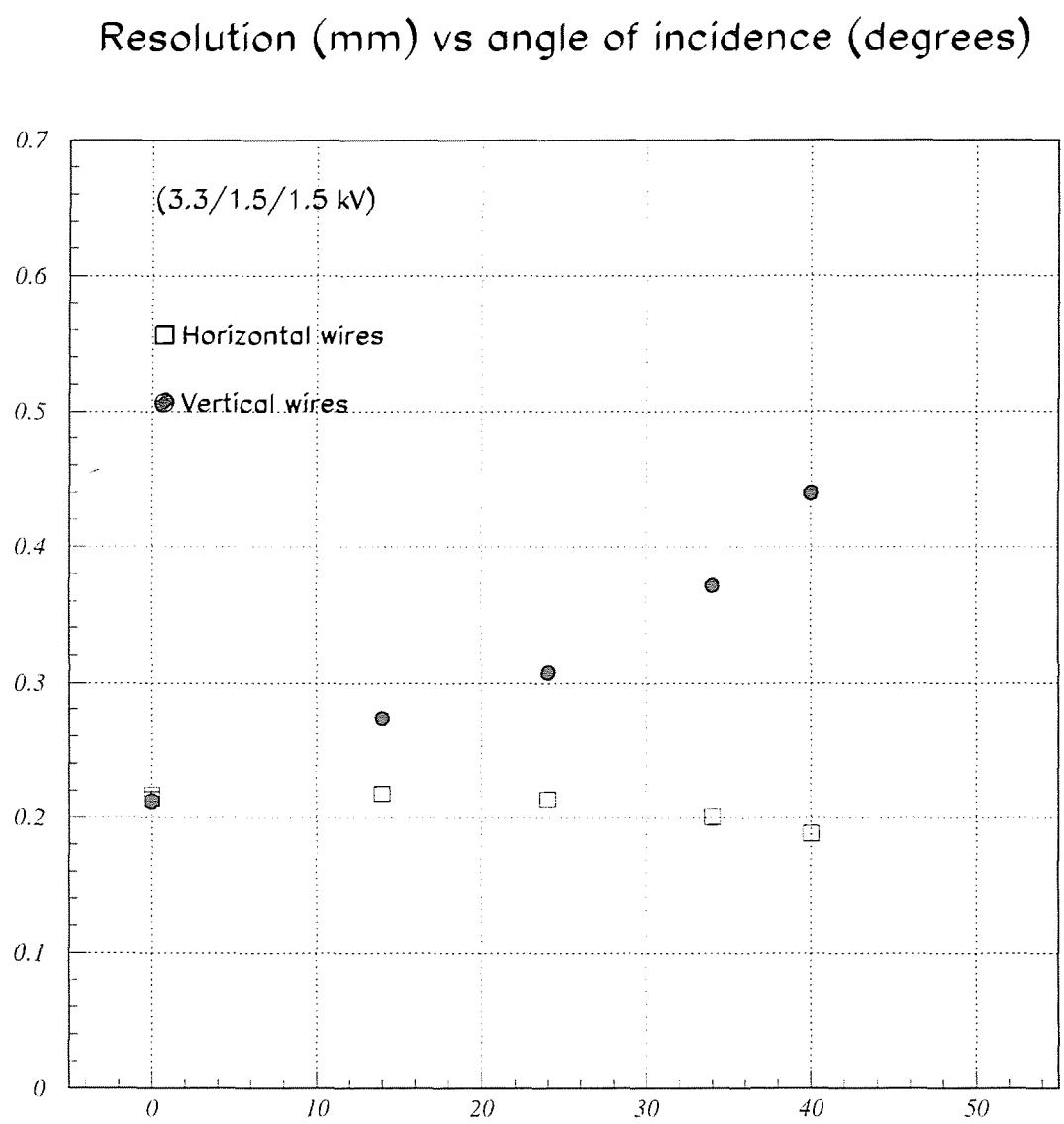

Figure 21: Global resolution, in mm, as a function of the angle of incidence, in degrees. No effect is seen in the horizontal superlayers as expected since the rotation was made around a vertical axis. In the case of vertical superlayers resolution becomes worse at bigger angles, partly due to the increase of deviations from linearities.

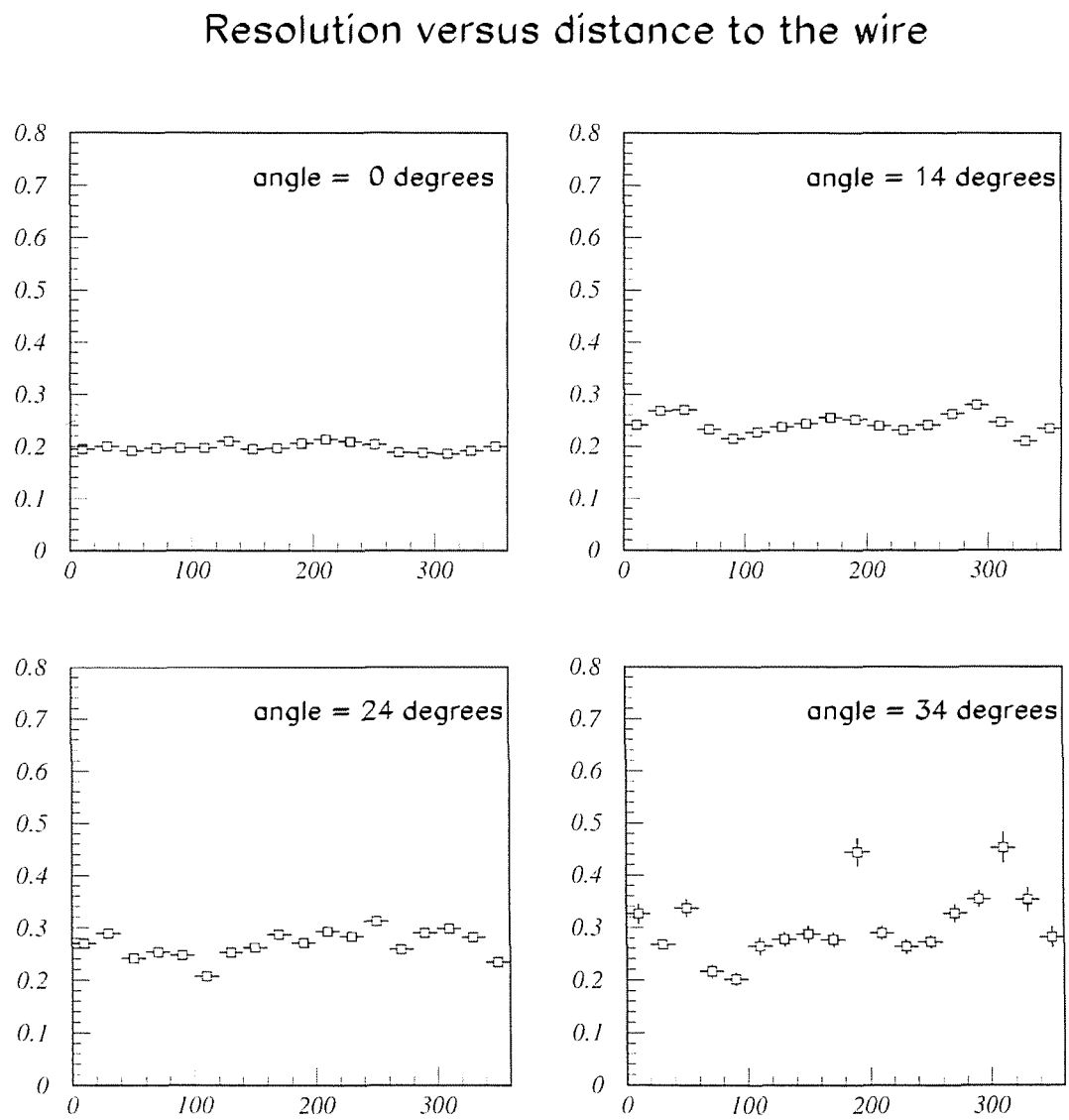

Figure 22: Single wire resolution, in mm, calculated in drift time bins of 20 ns each. Horizontal axis is the drift time bin value, in ns. Each plot corresponds to a given angle of incidence.

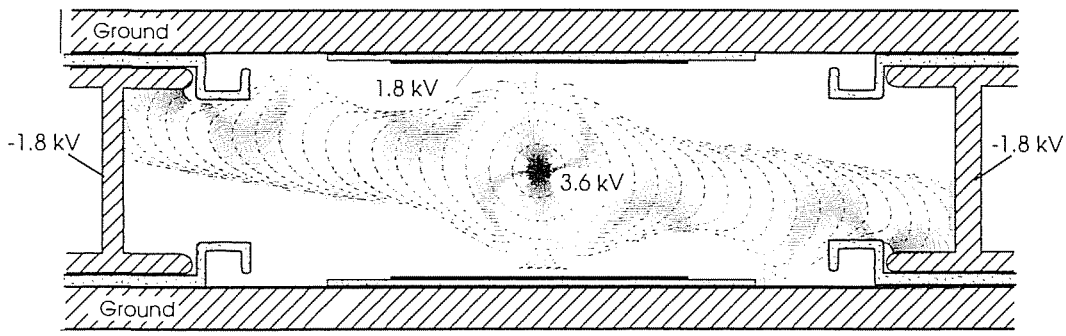

Figure 23: Effect of a B field of 0.45 Teslas parallel to the wires.

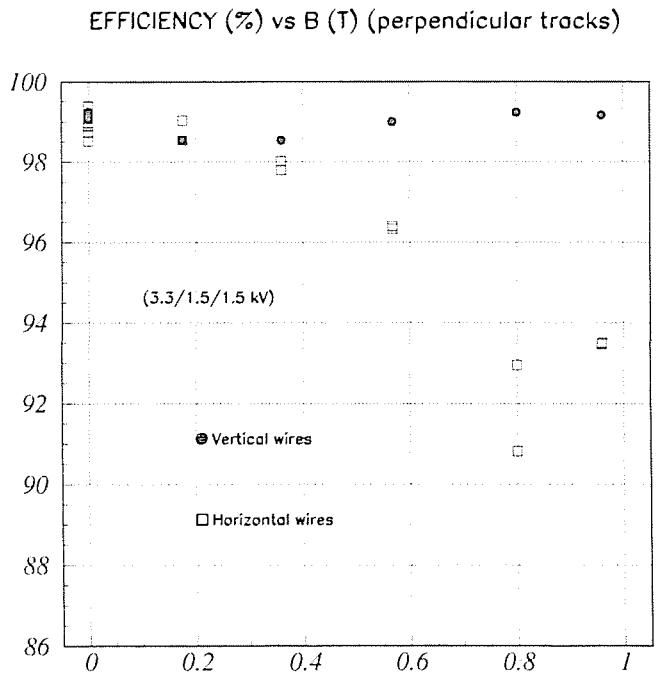

Figure 24: Single wire efficiency as a function of the B field value.

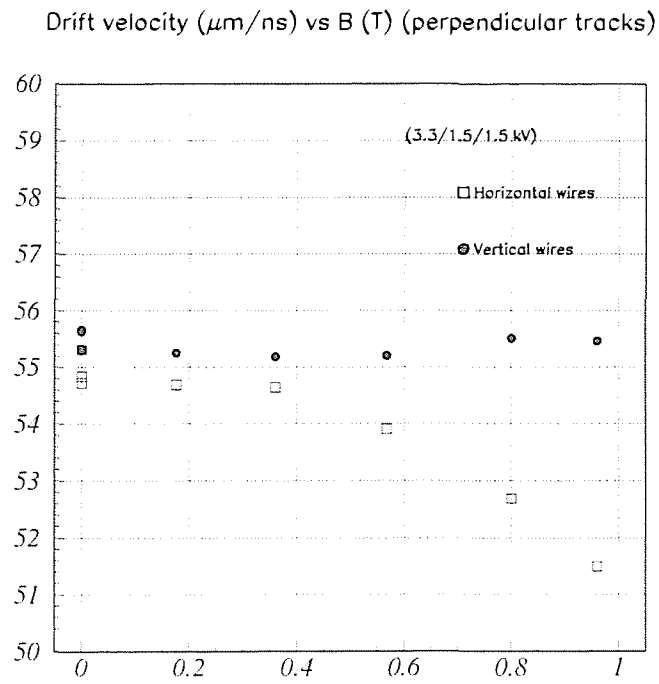

Figure 25: Drift velocity as a function of the B field value for perpendicular tracks.

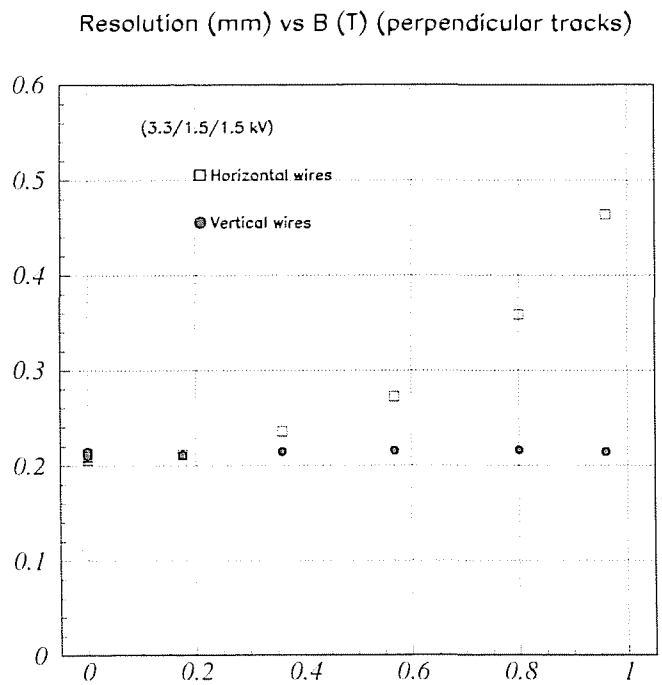

Figure 26: Single wire resolution as a function of the B field value for perpendicular tracks.

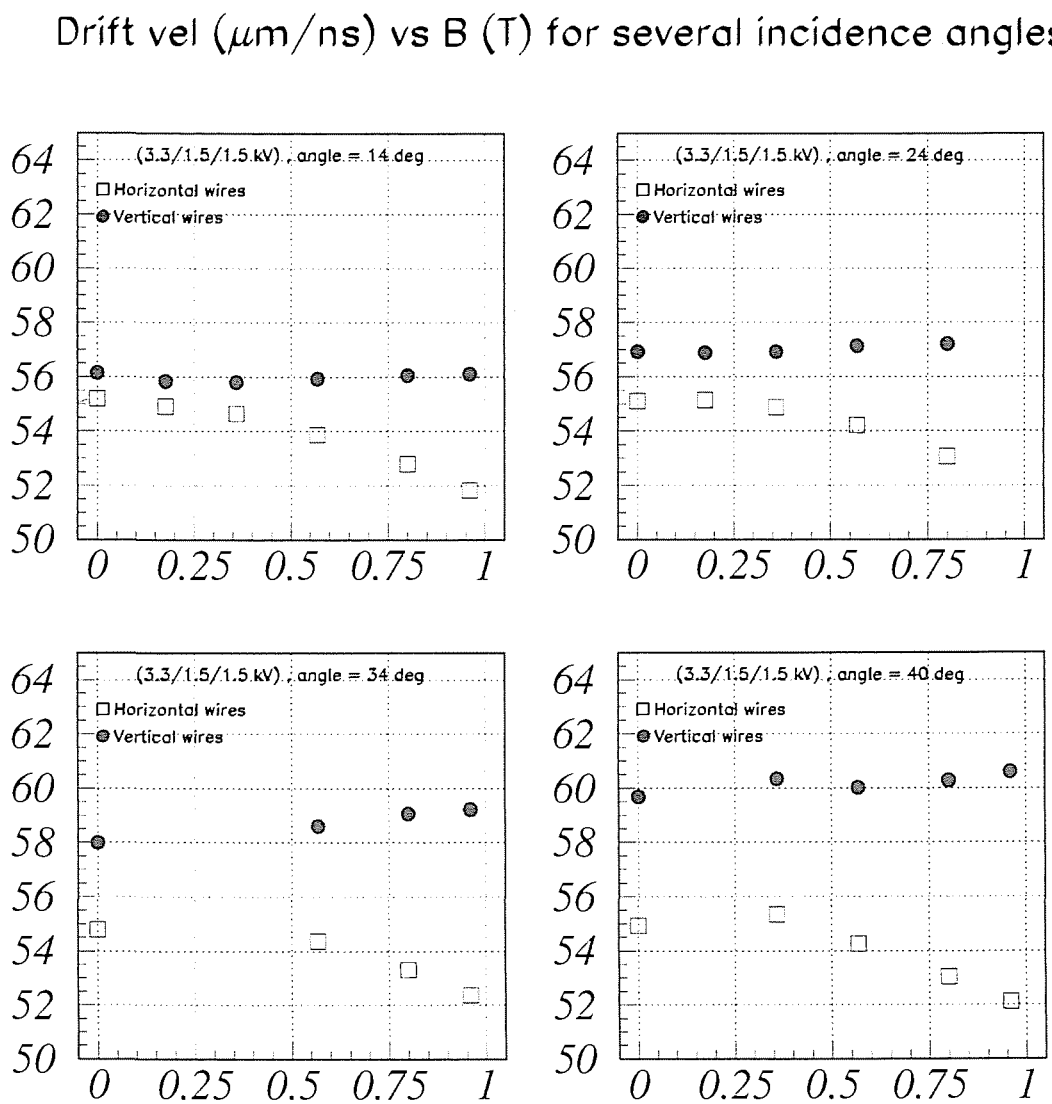

Figure 27: Here we show the effect of different B field values and different angles of incidence on the apparent drift velocity.

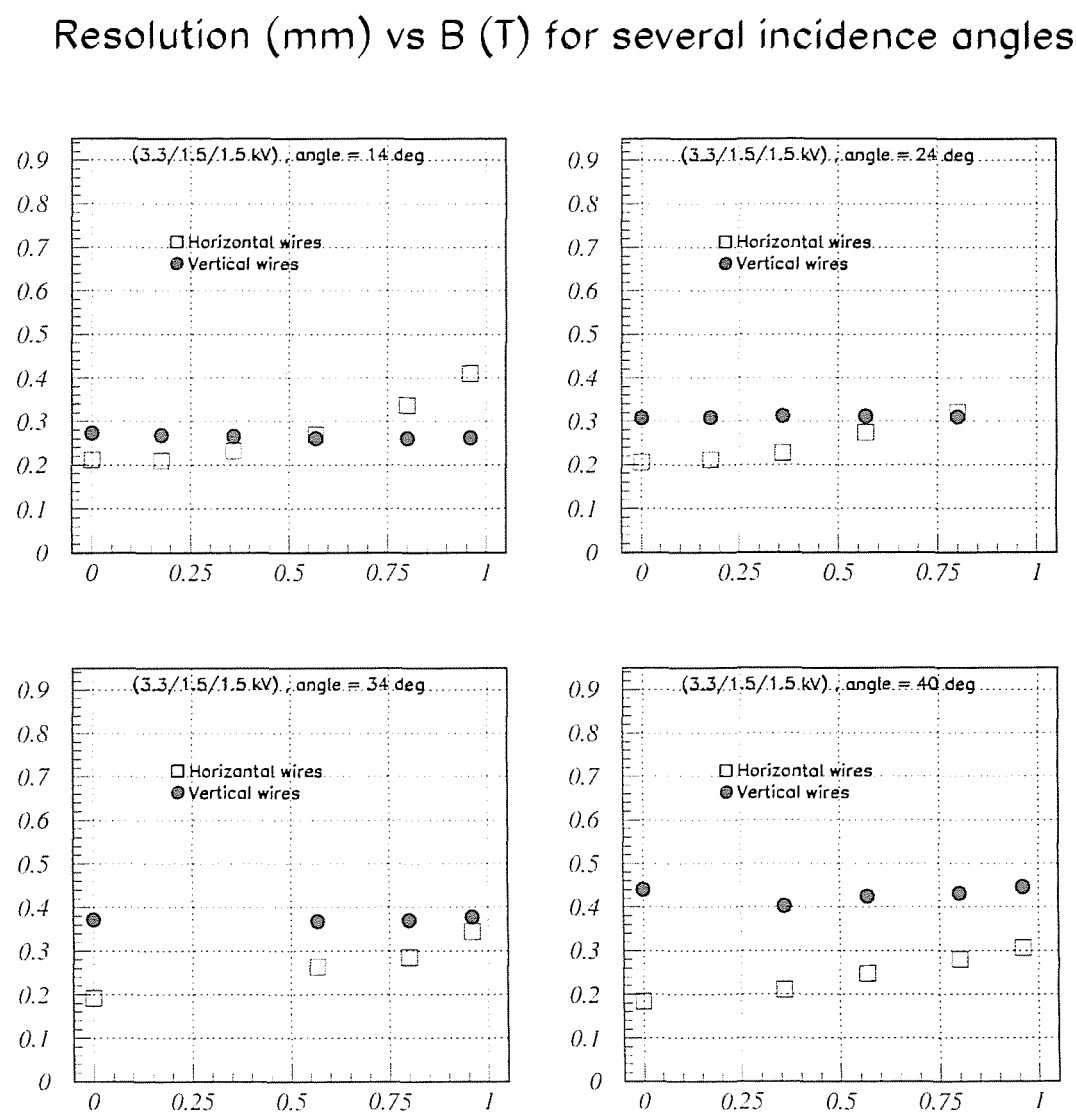

Figure 28: Here we show the effect of different B field values and different angles of incidence on the single wire resolution.